Volume 2 | Number 23 | 21 June 2014 | Pages 3559–3706

Journal of Materials Chemistry B

Materials for biology and medicine

www.rsc.org/MaterialsB

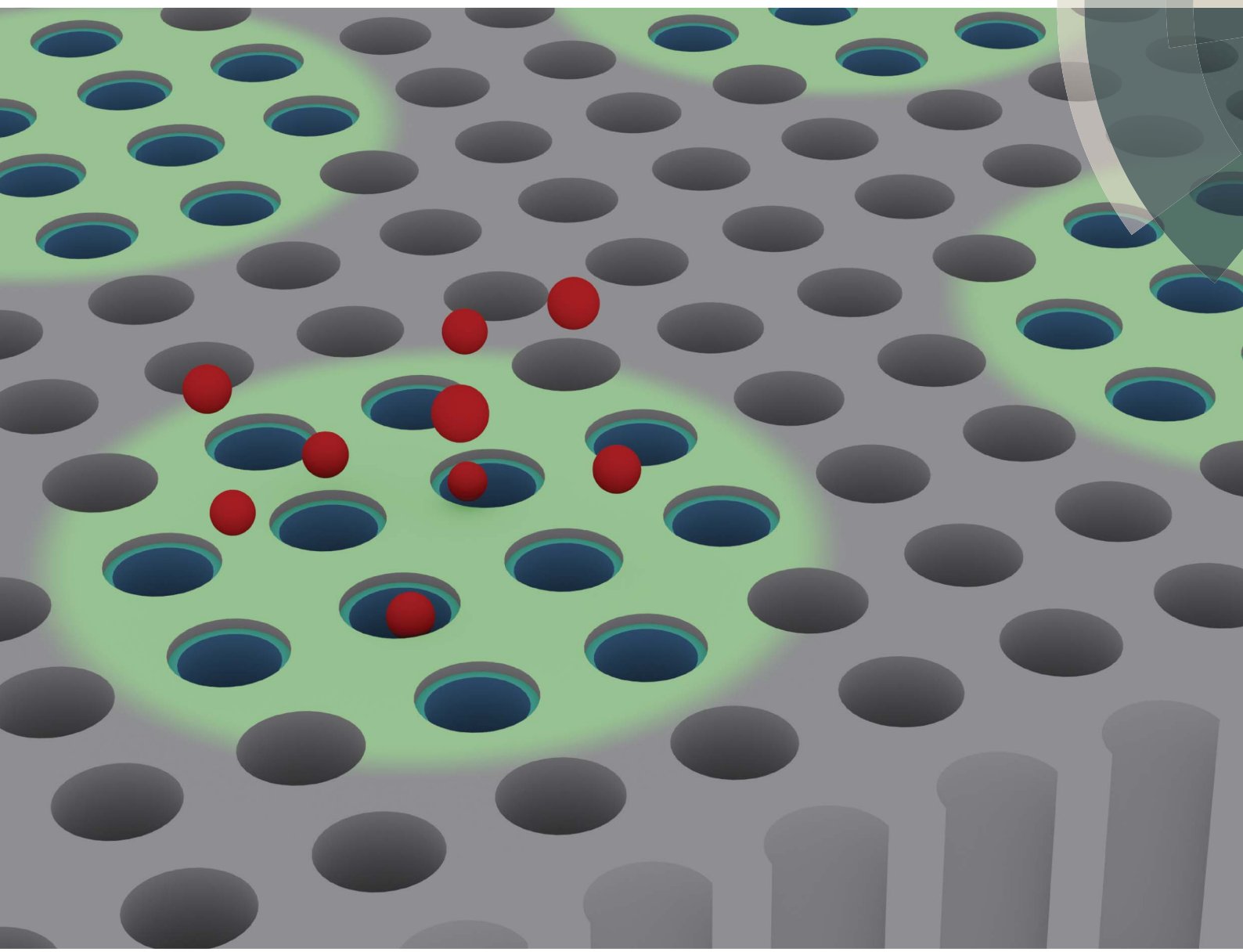

ISSN 2050-750X

ROYAL SOCIETY OF CHEMISTRY

PAPER

J. Justin Gooding *et al.*

Chemical patterning on preformed porous silicon photonic crystals: towards multiplex detection of protease activity at precise positions

Journal of Materials Chemistry B

PAPER

View Article Online
View Journal | View Issue

Cite this: J. Mater. Chem. B, 2014, 2, 3582

Chemical patterning on preformed porous silicon photonic crystals: towards multiplex detection of protease activity at precise positions†

Ying Zhu,[a] Alexander H. Soeriyadi,[a] Stephen G. Parker,[a] Peter J. Reece[b] and J. Justin Gooding*[a]

Received 20th February 2014
Accepted 30th March 2014

DOI: 10.1039/c4tb00281d

www.rsc.org/MaterialsB

Porous silicon (PSi) rugate filters modified with alkyne-terminated monolayers were chemically patterned using a combination of photolithography of photoresist and click chemistry. Two chemical functionalities were obtained by conjugating, *via* click reactions, ethylene glycol moieties containing two different terminal groups to discrete areas towards the exterior of a PSi rugate filter. The patterning of biological species to the functionalized surface was demonstrated through the conjugation of fluorescein isothiocyanate labelled bovine serum albumin (FITC-BSA). Fluorescence microscopy showed selective positioning of FITC-BSA at discretely functionalized areas. Meanwhile, the optical information from precisely defined positions on the patterned surface was monitored by optical reflectivity measurements. The optical measurements revealed successful step-wise chemical functionalization followed by immobilization of gelatin. Multiplex detection of protease activity from different array elements on the patterned surface was demonstrated by monitoring the blue shifts in the reflectivity spectra resulted from the digestion of gelatin by subtilisin. Precise information from both individual elements and average population was acquired. This technique is important for the development of PSi into a microarray platform for highly parallel biosensing applications, especially for cell-based assays.

Introduction

Porous silicon (PSi) photonic crystals are an ideal platform for label-free biosensing due to their high surface area, tunable pore size, biocompatibility and their flexibility in engineering optical properties and responses.[1–4] In addition, the hydride termination of as-prepared PSi can be modified using well-developed hydrosilylation chemistry, which significantly stabilizes the surface against silicon oxide growth, as well as enables the design of bio-recognition interfaces for biosensing.[5–7] As an interferometric biosensor, the response of a PSi photonic crystal is determined by changes in the effective bulk refractive index resulting from reactions/events occurring within the pore space.[8] Chemical derivatization or binding of analytes on the pore walls results in an increase in the average refractive index in the pore space, and hence an increase in the optical thickness. This increase in optical thickness is detected as a shift of the interference pattern towards higher wavelengths (red-shift). In contrast, the detachment or diffusion of materials out of the pore space leads to a blue shift of the interference pattern. Different PSi photonic structures (such as Fabry–Perot layers, resonant microcavities or rugate filters) with functionalized surface have been applied to detecting a variety of bioanalytes including antibody/antigen, enzyme, nucleic acids, and cells.[9–15]

To realise the potential of highly parallel PSi optical biosensors for multiplexed detection, new methods of microfabrication are required to achieve miniaturized and array-formatted structuring.[3] Firstly, because of the inhomogeneity in etching cell configurations and electrical field distribution in etching processes, heterogeneity in the optical properties occurs between different areas of the PSi surface. Instead of monitoring the average optical response from a broad area of PSi, it is much more accurate if the optical response from precise positions of PSi can be characterized. Fabrication of PSi into array structures and monitoring the response from each element of the array provides more precise and quantitative information from individual elements and the average population. Secondly, for microarray applications, it would be highly advantageous to be able to produce micropatterns of different chemical functionalities on discrete areas on the PSi surface, which can be further used for mediation of selective cell adhesion for cell-based assays or selective capture or detection of (bio)analytes. The strategies for PSi patterning fall into two categories. In the first one, a flat silicon wafer is patterned with

[a]School of Chemistry and the Australian Centre for NanoMedicine, University of New South Wales, Sydney 2052, Australia. E-mail: justin.gooding@unsw.edu.au
[b]School of Physics, University of New South Wales, Sydney 2052, Australia

† Electronic supplementary information (ESI) available: SEM images, XPS result and more optical reflectivity data. See DOI: 10.1039/c4tb00281d

masking materials by photolithography, and then PSi in defined regions is formed by local anodisation.[16–18] In the second one, the PSi structure is formed first, and then selectively modified with different functionalities. The advantages of the second approach are: (i) it provides more uniform optical properties across the surface as the PSi film is preformed, which is important for biosensing, and (ii) the homogenous porous surface rules out the uncertainty that surface topography may bring to the adhesion of analyte such as proteins and cells. There are several studies where patterning of a PSi surface with different chemical functionalities is performed. These strategies include the ones utilizing photolithographic techniques combined with silanization or hydrosilylation chemistries, and the ones that take advantage of the light-assisted hydrosilylation to directly pattern chemical functionalities on PSi surface without a lithographic hard mask.[19–21]

We have recently demonstrated the ability to chemically pattern PSi rugate filters on the internal pore space using microfabrication techniques in combination with click chemistry.[22] In this previous work, titanium was coated on the PSi surface before patterning so as to provide a protective layer to prevent the photoresist from penetrating into the pore space, which may prevent further chemical modification of the pores. However, we found later that the metal evaporation process used in this work had a potential to damage the monolayer on the external surface of PSi, which is due to the high temperature, kinetic energy of the metal atoms and radiation emitted from the heated source.[23] As a consequence, the coupling efficiency of the click reaction on the external surface was significantly reduced, which was observed by X-ray photoelectron spectroscopy (XPS). While providing excellent patterning of the internal pore structure, this loss of coupling efficiency is unfavourable for immobilization of biomolecules on the external surface of the PSi, which is essential for using PSi to selectively capture cells for cell-based sensing in our future work. Therefore, there is a need to develop a softer approach that allows chemical patterning on the external surface for selectively immobilization of biomolecules and functionalizing the inner pore walls for the loading of sensing agent.[24]

In the present work, we demonstrate the ability to produce patterns of chemical functionalities on PSi surfaces using a combination of photolithography of a photoresist and surface chemistry, where the need for a metal protective layer during the patterning step has been eliminated. Two chemical functionalities were obtained by conjugating ethylene glycol (EO) moieties containing different terminal groups to discrete areas on a PSi surface. Fluorescein isothiocyanate labelled bovine serum albumin (FITC-BSA) was incubated on the patterned surface, and the fluorescence patterns were observed by fluorescence microscopy. Meanwhile, the chemical patterning procedure was also characterized by optical reflectivity measurement. Finally, the inner pore walls were modified with gelatin, and the multiplex detection ability of the patterned PSi was demonstrated by monitoring the cleavage of gelatin at precise positions by a model enzyme – subtilisin.

Experimental section

Fabrication of PSi rugate filters

Mesoporous silicon rugate filters were prepared by galvanostatic anodisation of a boron-doped Si(100) wafer (1–1.5 mΩ cm, Siltronix, France) in a 30% (v/v) hydrofluoric acid ethanolic solution. The photonic structure of a PSi rugate filter was designed with 40 pairs of alternative high and low refractive index layers. Etching current densities were 21.1 and 23.7 mA cm^{-2}. After anodisation, the samples were rinsed in ethanol, dried under nitrogen gas, and stored under dry argon before further processing. The porosities of the two kinds of layer were 65.7 and 67.3%, which were obtained from simulation based on the Looyenga model. The thickness of the PSi film from highly doped wafer was *ca.* 8 μm and the average pore size was *ca.* 40 nm, as determined by scanning electron microscopy (Fig. S1, ESI†).

Modification of PSi rugate filters with 1,8-nonadiyne

Hydrosilylation of PSi samples was carried out using Schlenk line setup following a previously reported procedure.[24] Freshly-etched PSi rugate filters were immersed in deoxygenated 1,8-nonadiyne in a custom-made Schlenk flask. The sample was kept under an argon atmosphere while the Schlenk flask was immersed in an oil bath with the temperature set to 165 °C for 3 h. The flask was then opened to the atmosphere, and the sample was rinsed consecutively with copious amounts of redistilled dichloromethane and ethanol, blown dry under argon, and stored under argon before use or further processing.

Photoresist patterning on PSi surface *via* photolithography

The alkyne-functionalized PSi was then processed according to a standard photolithographic protocol as follows. The substrate was coated with positive photoresist AZ6612 (Microchemicals, Germany) by spin-coating at 4000 rpm for 30 s, and soft-baked at 95 °C for 1 min. The photoresist-coated substrate was irradiated with UV light for 7 s through a chrome-patterned photomask using a Quintel Q6000 mask aligner. Following UV exposure, the photoresist was immediately developed in AZ 400K developer (Microchemicals, Germany) for 30 s, rinsed with Milli-Q water for 30 s and dried under a stream of nitrogen gas. The photoresist was stripped after the first click reaction by rinsing the surface with copious amounts of acetone and isopropanol, and then dried under nitrogen gas.

Chemical patterning of PSi rugate filters

The photoresist-patterned PSi rugate filter was modified with different azido species in discrete regions by click reactions (Scheme 1). In the first click reaction, the following chemicals were added to a reaction tube before the photoresist patterned PSi sample was added: (i) azido species (10 mM in water), (ii) copper(II) sulphate pentahydrate (1 mol% relative to the azide), and (iii) sodium ascorbate (25 mol% relative to the azide). After the photoresist was stripped, the second click reactions followed a similar procedure except that water was replaced by a

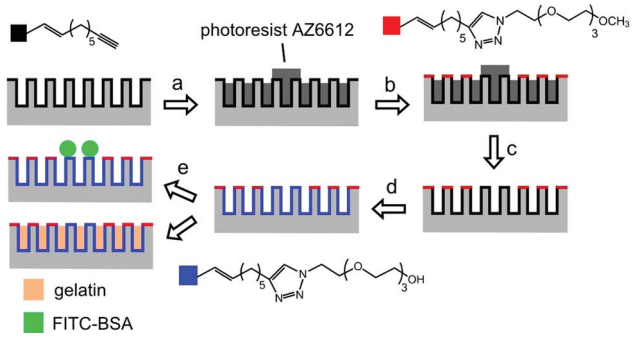

Scheme 1 Procedure for the patterning of discrete functionalities to PSi surface by a combination of photolithography of photoresist and click chemistry. Freshly etched PSi rugate filter was firstly functionalized with an alkyne-terminated monolayer. (a) An array of photoresist circles with diameter 100 μm was patterned on the PSi surface by photolithography. (b) The first azido species azido-EO_3–OCH_3 was attached on the upper region of pore structure in background regions by a click reaction with only water as the solvent. (c) Photoresist pattern was removed completely by rinsing the chip with acetone and isopropanol. (d) The second azido species azido-EO_3–OH was attached on the surface of spot regions and throughout the internal pore walls of the entire structure. (e) FITC-BSA was attached on chemically patterned PSi surface for fluorescence microscopy, or gelatin was filled in the internal pore space of the entire structure for protease assay.

mixture of water and ethanol (1 : 1). Both click reactions were carried out at room temperature for 19 h. After the reaction, the sample was immersed in 0.5 M hydrochloric acid to remove copper on the surface, rinsed with copious amounts of water and ethanol, and dried under a stream of argon.

Attachment of biological species to patterned PSi

For the covalent conjugation of biological species, the hydroxyl functionalized surface was activated *via* disuccinimidyl carbonate. Patterned PSi samples were placed into a reaction tube containing *N*,*N*′-disuccinimidyl carbonate (DSC, 0.1 M) and 4-dimethylaminopyridine (DMAP, 0.1 M) in dry acetonitrile for 20 h in the presence of activated molecular sieves (3 Å). The active carbonate samples were rinsed with ethyl acetate and dichloromethane and dried under a stream of argon. For FITC-BSA patterning, the sample was incubated in FITC-BSA solution (0.5 mg mL^{-1} in 1 × PBS) in the dark for 2 h, and rinsed thoroughly with 1 × PBS and 1 × PBS with 0.5% Tween 20. For protease assay, the same was incubated in gelatin solution (300 mg mL^{-1} in water, 90–110 bloom) at 37 °C for 3 h, casted at 4 °C for 30 min, and then rinsed thorough in 37 °C water to remove the unattached gelatin.

XPS measurements

XPS data was acquired using an ESCALAB 220iXL spectrometer with a monochromatic Al Kα source (1486.6 eV), hemispherical analyser, and multichannel detector. Spectra were recorded in normal emission with the analysing chamber operating below 1×10^{-9} mbar and selecting a spot size of ~1 mm^2. The incidence angle was set to 58° with respect to the analyser lens. The resolution of the spectrometer is *ca.* 0.6 eV as measured from the Ag 3d5/2 signal (full width at half-maximum) with a 20 eV pass energy. Survey scans were carried out over 1100–0 eV range with a 1.0 eV step size, a 100 ms dwell time, and analyser pass energy of 100 eV. High-resolution scans were run with 0.1 eV step size, dwell time of 100 ms, and the analyser pass energy set to 20 eV. After background subtraction using the Shirley routine, spectra were fitted with a convolution of Lorentzian and Gaussian profiles. All energies are reported as binding energies in eV and referenced to the C 1s signal (corrected to 285 eV).

Fluorescence microscopy

Fluorescence microscopy images were obtained from an inverted Leica DMIL epifluorescence microscope (Leica Microsystems Pty Ltd, USA), fitted with transmitted light LED back illumination and an EL6000 Fluoro system (mercury lamp). FITC fluorescence was detected with a GFP filter cube (excitation filter: BP470/40, dichroic mirror: 500, emission filter: 525/50). Images were observed under a 10 × NA0.22 air objective, and captured using ProgRes Capture Pro 2.7 software by an integrated ProgRes CFscan CCD camera (JENOPTIK laser, Optik, Systeme GmnH, Germany). The exposure time for recording the image was 5 s, and the gain factor was 1.0.

ImageJ 1.44p (National Institute of Health, USA) was used for the quantitative analysis of the fluorescence microscopy images obtained under the same instrumental setting (lamp intensity, magnification and exposure time). Mean grey values in 20 circular areas (diameter 80 μm) from both spot and background regions of the patterning images were measured to compare protein adsorptions between these two regions.

Optical characterization

Optical reflectivity spectra were measured in the visible and near-infrared at normal incidence using a custom-built optical arrangement. The setup incorporated a USB2000+ miniature fibre-optic spectrometer (Ocean Optics Inc.) and a fibre-coupled light source (Mikropack GmbH, Germany). The spectral resolution was 0.6 nm and the measurement spot size was *ca.* 80 μm. The optical arrangement was incorporated with a 2-axis (*X*–*Y*) automated stage (MS-2000, Applied Scientific Instrumentation). A custom software platform, driven by LabVIEW (National Instruments, TA), was used to process the spectra and provide a program for automatically moving of the stage. The peak position of each reflectivity spectrum was gathered by recording the wavelength corresponding to the maximum intensity after a polynomial fitting of the peak (Fig. S2, ESI†).

Protease assay

A gelatin-modified sample was incubated in 1 μM subtilisin solution in 1 × PBS at 37 °C in a circulating water bath. At various time points, the sample was removed from the solution, rinsed with water, and placed in a Petri dish filled with water. The reflectivity scanning was consistently started from the same spot, and the step size is the centre-to-centre distance of the spots in the array. The scanning angle was pre-adjusted to ensure the same spot regions were measured in every measurement.

Result and discussion

Chemical patterning of PSi pore structure by a combination of photolithography and click chemistry

The chemical patterning process is presented in Scheme 1. A freshly-etched PSi rugate filter was functionalized with an alkyne-terminated monolayer. A micro-sized array of photoresist circles (diameter 100 μm) was patterned on top of the PSi surface by a standard photolithography process. For flat surfaces, photoresist in the regions exposed to UV light can be completely removed after development process. However, this is impossible for PSi as the photoresist seeps into the porous structure. Therefore, only photoresist on the upper region of the pore structure was removed after photolithography. These regions are henceforth referred to as the 'background regions', while the regions with photoresist disks on top are referred to as the 'spot regions'. Thereafter, the first azido species with EO moiety and a methoxyl distal group (azido-EO_3–OCH_3) was attached on the upper region of the pore structure in background regions by a click reaction with only water as the solvent. The photoresist pattern was then removed completely by rinsing the chip thoroughly with acetone and isopropanol. The second azido species with the same EO moiety but terminated with a hydroxyl group (azideo-EO_3–OH) was then attached on the surface of spot regions and throughout the internal pore walls of the entire structure. XPS was used to characterize the surfaces that have undergone the same processes for acquiring the two functionalities in the spot and background regions for the patterning. Evidence of a successful click reaction of the EO derivatives on the upper region of pore structure in both the spot and background regions was provided by narrow scan of the C 1s and N 1s regions (Fig. S3, ESI†). Successful triazole formation was indicated by the presence of N 1s peak at ~401 eV fitted with a linear combination of two Gaussian functions with a 2 : 1 ratio of the integrated areas.

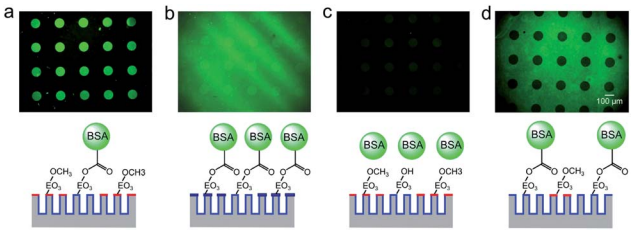

Fig. 1 Different designs of chemically patterned PSi surface with covalently attached or physisorbed FITC-BSA. (a) The background regions were modified with azido-EO_3–OCH_3, the spot regions were then modified with azido-EO_3–OH, and FITC-BSA was covalently attached to the spot regions. (b) The background regions were modified with azido-EO_3–OH, the spot regions was then modified with azido-EO_3–OH, and FITC-BSA was covalently attached to both the two regions. (c) The background regions were modified with azido-EO_3–OCH_3, the spot regions were then modified with azido-EO_3–OH, and FITC-BSA was physically adsorbed to the surface. (d) The background regions were modified with azido-EO_3–OH, the spot regions was then modified with azido-EO_3–OCH_3, and FITC-BSA was covalently attached to the background regions.

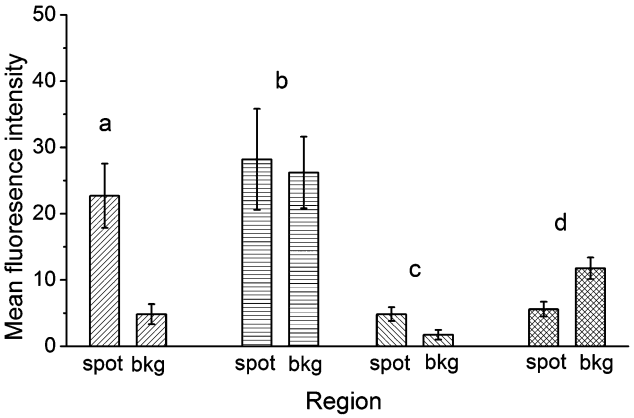

Fig. 2 Quantitative analysis of fluorescence intensity of images in Fig. 1 at different regions of patterns.

Incubation of FITC-BSA on micropatterned PSi surface

To visualize the patterned areas and demonstrate the ability to produce patterns of immobilized proteins, FITC-BSA was incubated on chemically patterned PSi surfaces. EO moieties have been shown to prevent nonspecific protein adsorption, and have been used in the preparation of PSi rugate filters for biosensing applications.[20,25,26] Fig. 1 displays the fluorescence microscopy images of FITC-BSA incubated on PSi surfaces patterned with different designs of chemical functionalities, and FITC-BSA was either covalently attached to hydroxyl group terminated regions (Fig. 1a, b and d) or physically adsorbed to the surface (Fig. 1c). Fig. 2 is a quantitative analysis of the fluorescence intensities in the corresponding images in Fig. 1. From Fig. 1a and d, it can be seen that the FITC-BSA was presented mostly on the hydroxyl terminated regions as compared with the methoxyl terminated regions, and the comparison of the fluorescence intensities shows there is a significant difference between the two regions (Fig. 2, column a and d). Fig. 1b shows the fluorescence image of FTIC-BSA covalently attached on the surface with the hydroxyl terminated monolayer attached in both the spot and background regions. As expected, the two regions have very similar amount of fluorescence (Fig. 2, column b), which excluded the possibility that the fluorescence patterning in Fig. 1a and d is due to the photolithographic process. In addition, the antifouling ability of the EO moiety was investigated. Fig. 1c and the corresponding fluorescence intensity analysis (Fig. 2, column c) show there is a significantly lower level of fluorescence from physically adsorbed FITC-BSA as compared with the covalently attached one from Fig. 1a, b and d. This result provides evidence that (1) FITC-BSA is only attached to the hydroxyl terminated surface by covalent bonding after DSC activation, and (2) EO functionality provides the surface with resistance toward nonspecific adsorption of FITC-BSA. This patterning method can be applied to selectively capture other bio-analytes for protein and cell-based microarrays.

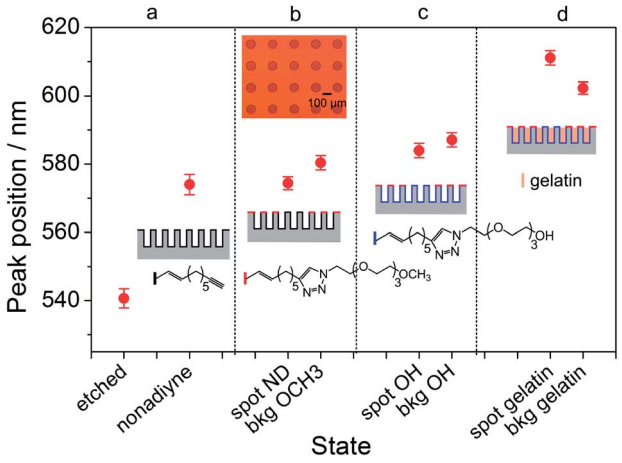

Fig. 3 Optical reflectivity from 100 data points after each step of modification on both spot and background regions of the patterned surface. The *x*-axis presents the state of the surface: 'etched' – freshly etched PSi; 'nonadiyne' – PSi after modification with nonadiyne (ND); 'spot ND' – spot regions with nonadiyne modified surface; 'bkg OCH_3' – background regions with azido-EO_3–OCH_3 modified surface; 'spot OH' – spot regions with azido-EO_3–OH modified surface; 'bkg OH' – background regions with azido-EO_3–OH modified surface; 'spot gelatin' – spot regions with gelatin modified surface; 'bkg gelatin' – background regions with gelatin modified surface. (a) The attachment of alkyne terminated monolayer resulted in 33 nm red shift of the peak position. (b) The attachment of azido-EO_3–OCH_3 in the background regions in the first click reaction resulted in 6.4 nm red shift in the background regions, while the spot regions have no shift; insert on the top shows an optical microscopy image of the chemically patterned PSi surface after the first click reaction. (c) The attachment of azido-EO_3–OH on the surface of spot regions and throughout the internal pore walls of the entire structure. There are 10 nm and 6.7 nm red shifts in the spot and background regions respectively. (d) The filling of gelatin into the pore structure leads to 27.1 nm and 15.2 nm red shifts on in the same spot and background regions.

Characterization of the chemical patterning by optical reflectivity

The fabricated PSi photonic crystal is a rugate filter structure, of which the spectrum consists of high-frequency small amplitude interference fringes and a single narrow-band high reflectivity Bragg peak (Fig. S2, ESI†). Chemical derivatization within the pore space leads to a red shift of the interference pattern, and can be characterized by the shift of peak position in the reflectivity spectrum. Fig. 3 shows the optical reflectivity data of PSi after hydrosilylation and each step of chemical patterning. The attachment of the alkyne-terminated monolayer resulted in a 33 nm red shift of the reflectivity peak position. After patterning of photoresist disks, the first azido species azido-EO_3–OCH_3 was attached in the background regions, followed by the complete removal of the photoresist. A visible pattern appeared after this process as shown in the insert of Fig. 3, which indicated a contrast in the optical signature of the spots and the background regions. The optical reflectivity setup incorporated with a *XY* automated stage was used to characterized the surface, and data was acquired by scanning 100 data points (a 10 × 10 array format) in the spot and background regions, respectively. It can be seen that the click reaction only occurred in the background region as determined by the 6.4 nm red shift to a new peak position at 580.4 ± 2.1 nm,‡ as compared to the alkyne-terminated surface in the spot regions (peak position 574.0 ± 3.0 nm). Generally, the red shift of a PSi film with the entire pore structure modified with the same azido species is usually 10–15 nm. The decrease in the red shift in the background region (6.4 nm) indicated that only part of the pore structure in the upper region was modified. On the other hand, the peak position of the spot regions remains the same at 574.4 ± 1.9 nm after photoresist removal, which is the same as the alkyne-modified surface before photolithography. This result indicates that photoresist has been completely removed and the photolithography process has little influence on the pore structure of PSi. It also indicates that the first click reaction did not occur in the spot regions, as they were blocked by photoresist during the reaction.

The second click reaction with azido-EO_3–OH was conducted after the complete removal of the photoresist. This reaction occurred on the surface of spot regions and throughout the internal pore walls of the entire structure. After the reaction, reflectivity was measured at the same spot and background regions as measured for the first modification. There are 10 nm and 6.7 nm red shifts in the spot and background regions respectively, which indicates the success of the modification. For the purpose of detecting the presence of active protease enzymes, gelatin was then covalently attached to the pore space, which serves as a substrate for protease enzymes. The filling of gelatin into the pore structure led to 27.1 nm and 15.2 nm red shifts in the same spot and background regions. The additional red shift in the spot regions indicated that there are more hydroxyl groups for the covalent attachment of gelatin compared to the background regions. Note that if the gelatin is not covalently attached we have observed that it washes out from the pores.

Multiplex detection of gelation digestion by subtilisin

PSi rugate filters have been used in our previous studies on detecting enzymatic activity by monitoring the blue shift resulted from substrate cleavage by enzymes.[11] Here, instead of obtaining a single data point from PSi that has been achieved in our previous work, the array-format patterned PSi chip was used to demonstrate the optical biosensor response in precise locations and the ability of multiplex detection. A gelatin-modified PSi rugate filter was incubated in a subtilisin solution at 37 °C. At different time points, the chip was removed from the subtilisin solution, rinsed with water to remove the cleaved peptide fragment and salt residue from buffer solution, and measured with an optical setup in water. Reflectivity peak positions were obtained in the same spot regions at each time point so as to rule out the uncertainty brought by the heterogeneity in the optical properties on different areas of PSi

‡ All the peak position data was presented as average ± standard deviation. Note red shifts indicate material of higher refractive index has entered the pores, which increases the average refractive index of the PSi. Blue shifts indicate the average refractive index of the PSi has decreased.

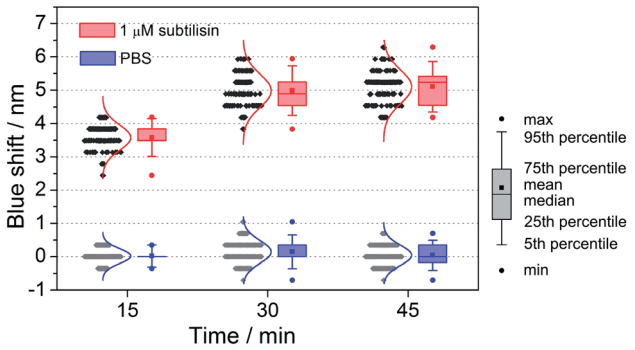

Fig. 4 Statistical distribution of optical response from 100 data points on the spot regions of a gelatin-loaded PSi incubated in subtilisin solution and PBS. The chip incubated in subtilisin solution showed an average blue shift of 3.5 nm immediately after 15 minutes and plateauing after 45 minutes with an average shift of 5 nm. However, the control sample showed little shift during the same time scale.

surface. Fig. 4 shows the optical response distribution from 100 data points (in a 10 × 10 array format) in the spot regions of gelatin-loaded PSi chips incubated in both 1 μM subtilisin solution and the control phosphate buffered saline (PBS). The apparent steps in the data are resulted from the resolution of the spectrometer. The chip incubated in subtilisin solution showed an average blue shift of 3.5 nm immediately after 15 min and plateauing after 45 min with an average shift of 5 nm. However, the control sample showed little shift during the same time scale, which provides evidence that the blue shift is caused by the protease cleavage. Fig. S4† presents examples of optical response from 5 array elements of the PSi chip incubated in subtilisin. Fig. S5† shows two examples of the spectral shifts with primary spectra. As the monitoring was carried out in an array format in the precisely defined regions, enzyme activity from each individual array element can be accurately acquired, and the statistics from the average population can also be obtained. This result is an important step for the development of PSi into a microarray platform for highly parallel biosensing applications.

Conclusion

In this work we have demonstrated a strategy for patterning different chemical functionalities in discrete regions of PSi rugate filter by a combination of photolithography and click reaction. The patterning of biological species to the functionalized surface was demonstrated through the conjugation of FITC-BSA to the substrate. The versatility of the described procedure makes this approach highly applicable to a wide range of biological species. As the patterned surface is recognizable through optical measurements, optical monitoring from precisely defined locations on PSi surface can be achieved. Multiplex detection of protease activity from different array elements on the patterned surface was demonstrated by monitoring blue-shifts in the reflectivity resulted from substrate cleavage by protease. Precise information from both individual elements and average population was acquired. This technique is important for the development of PSi into a microarray platform for selectively capturing biological species as well as highly parallel biosensing applications, especially for cell-based assays.

Acknowledgements

The authors thank the Australian Research Council (DP110102183), NHMRC (project grant APP1024723) and the NSW Node of the Australian National Fabrication Facility for support.

Notes and references

1 A. Jane, R. Dronov, A. Hodges and N. H. Voelcker, *Trends Biotechnol.*, 2009, **27**, 230–239.
2 S. Dhanekar and S. Jain, *Biosens. Bioelectron.*, 2013, **41**, 54–64.
3 B. Gupta, Y. Zhu, B. Guan, P. J. Reece and J. J. Gooding, *Analyst*, 2013, **138**, 3593–3615.
4 D. Fine, A. Grattoni, R. Goodall, S. S. Bansal, C. Chiappini, S. Hosali, A. L. van de Ven, S. Srinivasan, X. Liu, B. Godin, L. Brousseau, I. K. Yazdi, J. Fernandez-Moure, E. Tasciotti, H.-J. Wu, Y. Hu, S. Klemm and M. Ferrari, *Adv. Healthcare Mater.*, 2013, **2**, 632–666.
5 J. M. Buriak, *Chem. Commun.*, 1999, 1051–1060.
6 J. H. Song and M. J. Sailor, *Comments Inorg. Chem.*, 1999, **21**, 69–84.
7 K. A. Kilian, T. Böcking and J. J. Gooding, *Chem. Commun.*, 2009, 630–640.
8 Y. Zhao, X. Zhao and Z. Gu, *Adv. Funct. Mater.*, 2010, **20**, 2970–2988.
9 K. P. S. Dancil, D. P. Greiner and M. J. Sailor, *J. Am. Chem. Soc.*, 1999, **121**, 7925–7930.
10 S. O. Meade, M. Y. Chen, M. J. Sailor and G. M. Miskelly, *Anal. Chem.*, 2009, **81**, 2618–2625.
11 K. A. Kilian, L. M. H. Lai, A. Magenau, S. Cartland, T. Böcking, N. Di Girolamo, M. Gal, K. Gaus and J. J. Gooding, *Nano Lett.*, 2009, **9**, 2021–2025.
12 M. M. Orosco, C. Pacholski and M. J. Sailor, *Nat. Nanotechnol.*, 2009, **4**, 255–258.
13 A. Soeriyadi, B. Gupta, P. Reece and J. J. Gooding, *Polym. Chem.*, 2014, **5**, 2333–2341.
14 H. Ouyang, M. Christophersen, R. Viard, B. L. Miller and P. M. Fauchet, *Adv. Funct. Mater.*, 2005, **15**, 1851–1859.
15 L. M. Bonanno and L. A. DeLouise, *Anal. Chem.*, 2009, **82**, 714–722.
16 C. Chiappini, E. Tasciotti, J. R. Fakhoury, D. Fine, L. Pullan, Y.-C. Wang, L. Fu, X. Liu and M. Ferrari, *ChemPhysChem*, 2010, **11**, 1029–1035.
17 B. S. Flavel, M. J. Sweetman, C. J. Shearer, J. G. Shapter and N. H. Voelcker, *ACS Appl. Mater. Interfaces*, 2011, **3**, 2463–2471.
18 L. Chen, Z.-T. Chen, J. Wang, S.-J. Xiao, Z.-H. Lu, Z.-Z. Gu, L. Kang, J. Chen, P.-H. Wu, Y.-C. Tang and J.-N. Liu, *Lab Chip*, 2009, **9**, 756–760.
19 M. J. Sweetman, C. J. Shearer, J. G. Shapter and N. H. Voelcker, *Langmuir*, 2011, 9497–9503.

20 M. J. Sweetman, M. Ronci, S. R. Ghaemi, J. E. Craig and N. H. Voelcker, *Adv. Funct. Mater.*, 2012, **22**, 1158–1166.
21 M. P. Stewart and J. M. Buriak, *Angew. Chem., Int. Ed.*, 1998, **37**, 3257–3260.
22 Y. Zhu, B. Gupta, B. Guan, S. Ciampi, P. J. Reece and J. J. Gooding, *ACS Appl. Mater. Interfaces*, 2013, **5**, 6514–6521.
23 H. Haick and D. Cahen, *Prog. Surf. Sci.*, 2008, **83**, 217–261.
24 B. Guan, S. Ciampi, G. Le Saux, K. Gaus, P. J. Reece and J. J. Gooding, *Langmuir*, 2011, **27**, 328–334.
25 K. A. Kilian, T. Bocking, S. Ilyas, K. Gaus, W. Jessup, M. Gal and J. J. Gooding, *Adv. Funct. Mater.*, 2007, **17**, 2884–2890.
26 M. Mrksich, *Chem. Soc. Rev.*, 2000, **29**, 267–273.